

Inelastic Stress/Strain Behavior near Circumferential Notch Root of 2·1/4Cr-1Mo Steel at 600°C

Tatsuo INOUE

Kyoto Univ., Kyoto, Japan

Shoji IMATANI

Kyoto Inst. Tech., Kyoto, Japan

Yoshio FUKUDA

Hitachi Ltd., Hitachi, Japan

Kazunari FUJIYAMA

Toshiba Corp., Yokohama, Japan

Kazumi AOTO

Power React. Nucl. Fuel Devel. Co., Tokyo, Japan

Kenji TAMURA

Kawasaki Heavy Ind. Ltd., Tokyo, Japan

1 INTRODUCTION

In order to evaluate the material response of high temperature machine components, sophisticated scheme for stress analysis has to be established. The Subcommittee on Inelastic Analysis and Life Prediction of High Temperature Materials (IALIPS), the Society of Materials Science, Japan (JSMS), whose members are listed in the footnote of the report A-1, has been performing a cooperative research work on the examination of existing inelastic constitutive equations under plasticity-creep interaction conditions. And creep-fatigue life prediction has been carried out based on the simulated stress-strain curve as well as on the experimental data. Some of the results have been reported so far (Inoue et al. 1989a,b, 1991a,b).

The subcommittee has extended its activity to finite element analysis of circumferential notch cylinders. Following a series of comparative study concerning uniform stress-strain responses in the reports A-1 and A-II, this paper B-I deals with the FEM evaluation of the notched component. Ten types of inelastic constitutive equations within eight categories are used in the finite element analysis, and four types of loading patterns are examined for two kinds of notch shape. The local strain response near the notch root is compared with the experimental results by means of a capacitance type extensometer. The creep-fatigue life prediction for the above is discussed in the report B-II.

2 EXPERIMENTAL PROCEDURE

The test material employed throughout this cooperative research work is a normalized and tempered 2·1/4Cr-1Mo steel (SA287, GR.22). The material is shaped into circumferential notch specimens as shown in Fig.1 where two kinds of notch are presented: one is a blunt notch with an elastic stress concentration factor K_t of 1.5 and the other has the factor of 3.0.

An electric capacitance type extensometer "Strain-Pecker" is spot-welded to the notch root with a gauge length of about 0.5mm to measure a local strain ϵ_{sp} , and another Strain-Pecker is also used to control a global strain ϵ_{GL} between the gauge length of 30mm. Therefore average strains between these gauge lengths are measured and controlled, so we compare the experimental results with the mean strain converted from the axial displacement of the corresponding node in FEM. This extensometer is available for high temperature utilization up to 700°C. The experiment was carried out at 600°C.

SMIRT 11 Transactions Vol. L (August 1991) Tokyo, Japan, © 1991

3 BENCHMARK PROBLEMS

Table 1 summarizes the loading condition of the benchmark problems which are briefly described as follows:

- I. Creep loading under the nominal stress $\sigma_{nom}=120\text{MPa}$ which is defined as the axial force divided by the minimum cross section.
 - II. Fast-fast cyclic straining at the strain rate $\dot{\epsilon}_{GL}=0.025\%/s$ with the strain range $\Delta \epsilon_{GL}=0.2\%$.
 - III. Slow-slow cyclic straining at $\dot{\epsilon}_{GL}=0.001\%/s$ with the same strain range $\Delta \epsilon_{GL}=0.2\%$.
 - IV. Fast-fast cyclic straining with tension hold for $t_h=600s$.
- The experiments were continued until rupture except for the problem I in order to get failure lives. Those data are adopted in the creep-fatigue life prediction schemes in B-II.

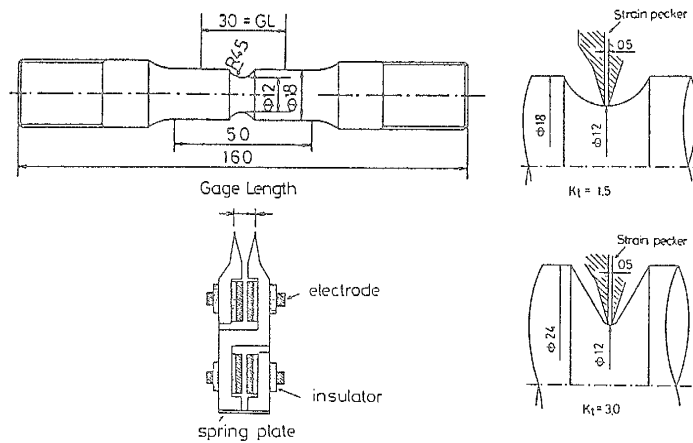


Fig. 1 The notched specimens and the extensometer "Strain-Pecker".

Table 1 Summary of the benchmark problems.

Problem	Loading Pattern	Condition	Experiment	Analysis
I	σ_{nom} Creep	$\sigma_{nom} = 120 \text{ MPa}$	$\sim 200 \text{ h}$	$\sim 100 \text{ h}$
II	ϵ_{GL} Fast-fast	$\Delta \epsilon_{GL} = 0.2 \%$ $\dot{\epsilon}_{GL} = 0.025 \%/s$	to rupture	$\sim N=10$
III	ϵ_{GL} Slow-slow	$\Delta \epsilon_{GL} = 0.2 \%$ $\dot{\epsilon}_{GL} = 0.001 \%/s$	to rupture	$\sim N=10$
IV	ϵ_{GL} Fast-fast with tension hold	$\Delta \epsilon_{GL} = 0.2 \%$ $\dot{\epsilon}_{GL} = 0.025 \%/s$ $t_h = 600 \text{ s}$	to rupture	$\sim N=10$

4 CONSTITUTIVE MODELS EXAMINED

Ten kinds of inelastic constitutive models are examined for the analysis of the benchmark problems. They are:

- (1)-(3) Superposition models (A), (C), and (D),
- (4) Modified superposition model,
- (5) Chaboche model,
- (6) Miller model,
- (7) Krempl model,
- (8) Bodner model,
- (9) Ohno-Murakami model,
- (10) Endochronic model.

The marks (A), (C), and (D) of the superposition model indicate that each model is employed for the analysis by different researchers and follow the nomenclature in the report A-I where the validity of these models is discussed within a uniform stress state of combined tension/compression and torsion on thin walled tubular specimens. The models are introduced to the FEM code by each researcher or by each institution.

5 RESULTS OF ANALYSES AND EXPERIMENTS

5.1 Creep deformation at notch root

Figure 2 implies a comparison of temporal strain levels during the creep deformation problem up to 100h. The circles and the square marks mean the local strain ϵ_{SP} at the time of 100h and 50h respectively, and the triangular marks indicate the global strain ϵ_{GL} at 100h. The unified constitutive models have much variation in both strains. That is to say that the endochronic model shows a good agreement with the experiment while the Krempl model overestimates the global strain. Moreover the models by Chaboche, Miller and Bodner hardly simulate the progress of the local strain. The superposition models and the modified superposition model give slightly less strain accumulation than the experiment.

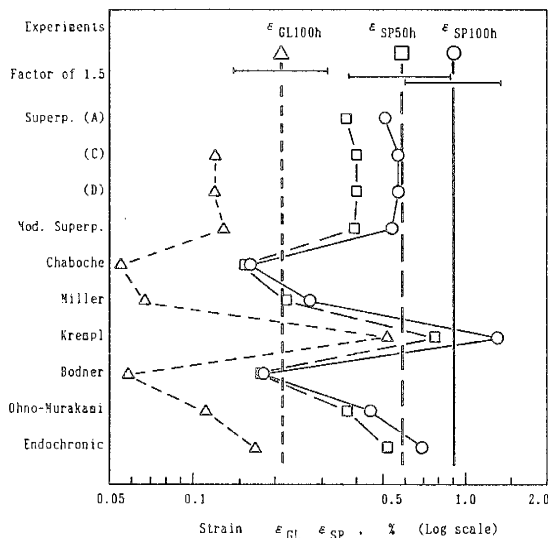


Fig. 2 Progressive strains during the creep deformation.

5.2 Stress-strain response under cyclic straining

Examples of the hysteresis loop for the problem III take place in Fig. 3 where Fig.(a) represents the experimentally obtained stress-strain response and Figs. (b), (c) and (d) respectively correspond to the analytical results by the Chaboche model, the Miller model and the Bodner model. Although the scale of the figures differs from each other so that we can hardly compare the results, the strain ranges seem to fit the experiment well. Actually it is reported that most models simulate the satisfactory strain concentration for any case of the strain patterns.

Figure 4 represent the nominal stress range for all the cases of cyclic straining. As for the fast-fast straining, most models provide good results for both notch shapes. However, the Ohno-Murakami model underestimates the stress range for the blunt notch. On the contrary, the stress responses of slower cycles reveal much variation. The unified models, e.g. the Chaboche model, the Bodner model and the Ohno-Murakami model, may have a capability of describing the rate dependence of the notched component while the superposition models do not predict this effect so accurately.

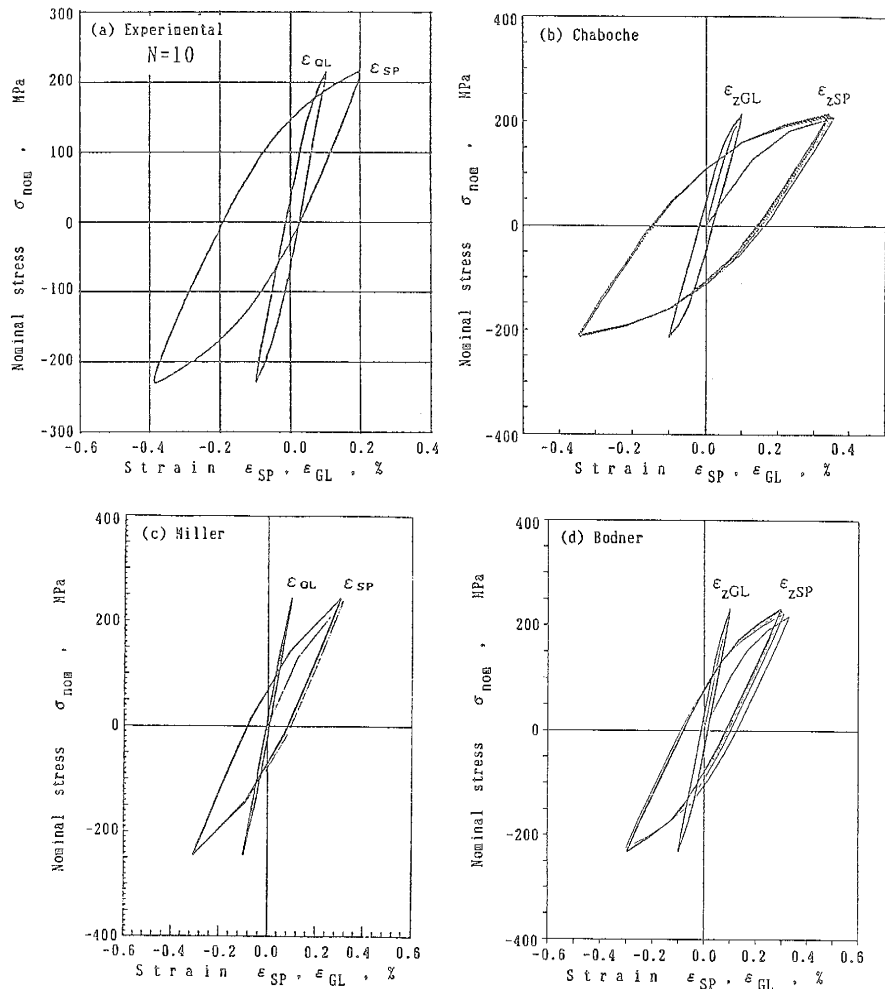


Fig. 3 Hysteresis loops under the slow-slow cyclic straining.

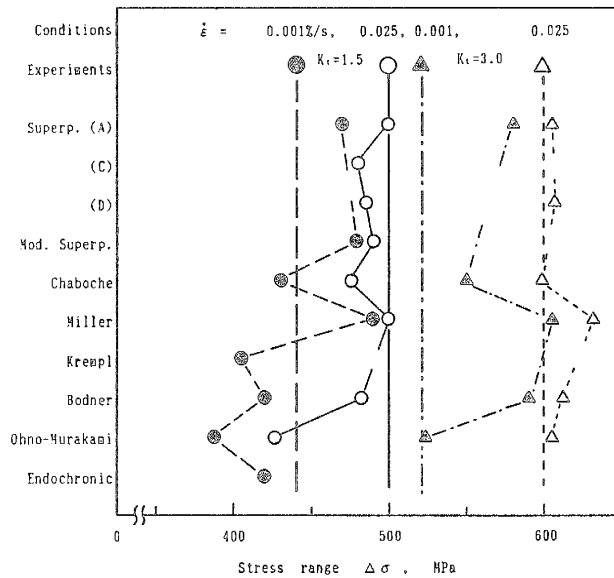


Fig. 4 The nominal stress ranges of the cyclic straining.

5.3 Stress distribution under the tension hold

When the tensile strain is kept constant for 600s in the problem IV, the local strain ϵ_{sp} makes progress whereas the axial stress shows a gradual drop due to relaxation. It implies that the stress distribution may vary with time. Figure 5 indicates the axial stress distribution during the tension hold by the Ohno-Murakami model as an example, in which Fig.(a) corresponds to the beginning of the hold and Fig.(b) is at the time $t_h=600s$. The axial stress is relaxed in the whole region, particularly at the notch root. The maximal stress level appears in a little inner part from the notched surface.

6 CONCLUSION

Finite element analysis was implemented on circumferential notch cylinders, and the experimental verification was also carried out using an extensometer Strain-Pecker. Such an FEM analysis enables us to understand a profound insight of the inelastic response of high temperature materials. It is then desirable to develop a sophisticated scheme for inelastic analysis and life prediction, based on the results obtained throughout this cooperative research work.

Acknowledgment

A part of this work was supported by the Ministry of Education, Japan, as Grant-in-Aid for cooperative research A (No.01302026). The test material was provided by Kawasaki Steel Co. LTD.

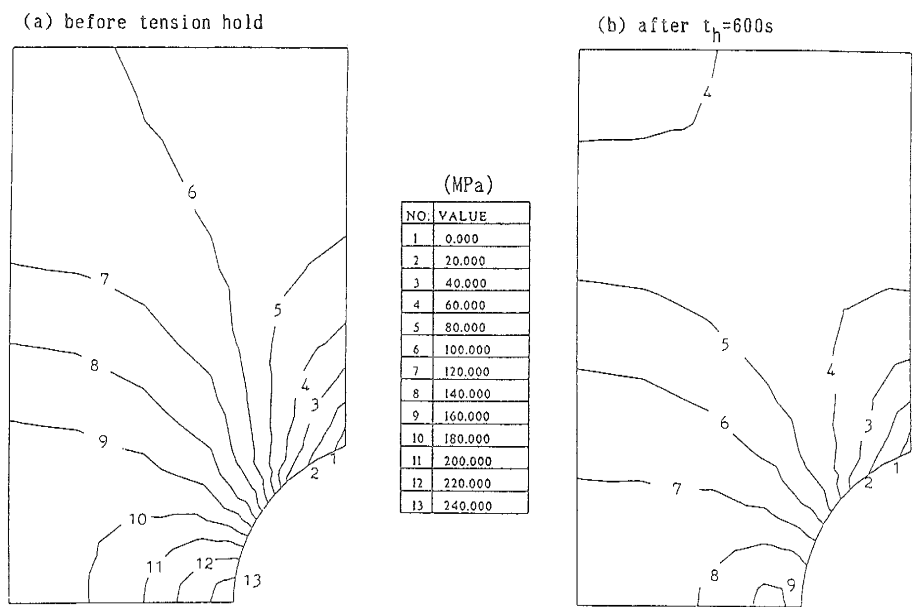


Fig. 5 Axial stress distribution by the Ohno-Murakami model.

REFERENCES

Inoue, T., Ohno, N., Suzuki, A. and Igari, T. (1989a). Evaluation of Inelastic Constitutive Models under Plasticity-creep Interaction for 2·1/4Cr-1Mo Steel at 600° C, Nucl. Eng. Des., Vol. 114, pp.295-309.

Inoue, T., Igari, T., Okazaki, M., Sakane, M. and Tokimasa, K. (1989b). Fatigue-creep Life Prediction of 2·1/4Cr-1Mo Steel by Inelastic Analysis, Nucl. Eng. Des., Vol. 114, pp.311-321.

Inoue, T., Yoshida, F., Ohno, N., Kawai, M. and Niitsu, Y. (1991a). Evaluation of Inelastic Constitutive Models under Plasticity-creep Interaction in Multi-axial Stress State, Nucl. Eng. Des. (in print).

Inoue, T., Okazaki, M., Igari, T., Sakane, M. and Kishi, S. (1991b). Evaluation of Fatigue-creep Life Prediction Methods in Multiaxial Stress State, Nucl. Eng. Des. (in print).